How does tissue regeneration influence the mechanical behavior of additively manufactured porous biomaterials?

Hedayati, R.; Janbaz, S.; Sadighi, M.; Mohammadi-Aghdam, M.; Zadpoor, A. A.

DOI
10.1016/j.jmbbm.2016.10.003

Publication date
2017

Document Version
Accepted author manuscript

Published in
Journal of the Mechanical Behavior of Biomedical Materials

Original article

How does tissue regeneration influence the mechanical behavior of additively manufactured porous biomaterials?

R. Hedayati[1,2*], S. Janbaz[2], M. Sadighi[1], M. Mohammadi-Aghdam[1], A.A. Zadpoor[2]

[1]*Department of Mechanical Engineering, Amirkabir University of Technology (Tehran Polytechnic), Hafez Ave, Tehran, Iran*
[2]*Department of Biomechanical Engineering, Faculty of Mechanical, Maritime, and Materials Engineering, Delft University of Technology (TU Delft), Mekelweg 2, 2628 CD, Delft, The Netherlands*

[1] Corresponding author, email: r.hedayati@tudelft.nl, rezahedayati@gmail.com, rezahedayati@aut.ac.ir, Tel: +31-15-2781021.

Abstract

Although the initial mechanical properties of additively manufactured porous biomaterials are intensively studied during the last few years, almost no information is available regarding the evolution of the mechanical properties of implant-bone complex as the tissue regeneration progresses. In this paper, we studied the effects of tissue regeneration on the static and fatigue behavior of selective laser melted porous titanium structures with three different porosities (i.e. 77, 81, and 85%). The porous structures were filled with four different polymeric materials with mechanical properties in the range of those observed for *de novo* bone (0.7 GPa< E <1.5 GPa) to simulate bone tissue regeneration into their pores. The static mechanical properties and fatigue behavior (S-N) curves of as-manufactured and filled porous structures were then determined. The static mechanical properties and fatigue life (including endurance limit) of the porous structures were found to increase by factors 2-7, even when they were filled with polymeric materials with relatively low mechanical properties. The relative increase in the mechanical properties was much higher for the porous structures with lower porosities. Moreover, the increase in the fatigue life was more notable as compared to the increase in the static mechanical properties. Such large values of increase in the mechanical properties with the progress of bone tissue regeneration have implications in terms of mechanical stimulus for bone tissue regeneration.

Keywords: Bone regeneration; porous biomaterials; additive manufacturing; fatigue properties.

1. INTRODUCTION

Optimum tissue regeneration performance of bone substituting materials is dependent, among other factors, on their mechanical behavior. Biomaterials with insufficient mechanical properties cannot provide enough mechanical support for bone tissue regeneration particularly in load bearing applications, while overly stiff biomaterials could hinder bone tissue regeneration through the stress shielding phenomenon. It is the therefore important to carefully choose the mechanical properties of biomaterials aimed for bone tissue regeneration. Given the repetitive nature of musculoskeletal loads, not only the static mechanical properties but also the fatigue behavior of bone substituting biomaterials needs to be properly adjusted for optimum tissue regeneration performance [1].

Additively manufacturing (i.e. 3D printing) [2, 3] enables adjustment of both static [4-8] and fatigue [9, 10] properties of porous biomaterials through rational design of the micro-architecture of the porous structure such as the choice of repeating unit cell type and adjustment of the dimensions of the unit cells. A number of researches have been dedicated to the investigation of mechanical properties of bone substitute biomaterials under static [11, 12] and fatigue loads [13-15]. Computational models [11, 16] could be used to predict the mechanical properties that result from any given design of the micro-architecture. Coupled with optimization algorithms, the computational models could determine the specification of the micro-architecture that gives rise to the desired mechanical properties. Given all this design flexibility, the most important question is ‘what are the desired mechanical properties’?

The most straightforward answer [1, 17] to the above-mentioned question has usually been ‘the mechanical properties of the native tissue’. The idea behind this answer is that the mechanical properties of scaffolds should resemble those of the native tissue they intend to ultimately

replace. Although this answer provides a good starting point, it has to be noted that the ultimate mechanical properties of the native tissue are not necessarily the ones that optimize the tissue regeneration performance of scaffolds [1, 17]. Furthermore, the mechanical behavior of porous biomaterials might drastically change as the tissue regeneration process progresses. Two factors contribute to the changes in the mechanical behavior of porous biomaterials including biodegradation of the scaffold and the regeneration of the tissue inside the porous structure that carries a gradually increasing portion of the applied load.

There is very limited experimental data available in the literature as to how the mechanical behavior of rationally designed and additively manufactured porous biomaterials change with the progress of the bone tissue regeneration process. That is partially due to the complexity of the problem at hand. There are many physical phenomena and design parameters that could play a role in this regard. In this study, we carefully designed experiments that could provide answers to some of the above-mentioned questions. We focused on selective laser melted porous titanium biomaterials aimed for bone tissue regeneration to exclude the effects of bio-degradation and focus on the effects of tissue regeneration. Porous scaffolds were additively manufactured with three different porosities. The additively manufactured scaffolds were filled with four polymeric materials whose mechanical properties simulated those of bone at various stages of maturation and at various anatomical locations. The mechanical properties of the scaffolds and polymeric materials were determined individually before filling the scaffolds with polymeric materials. The static mechanical properties and fatigue behavior (S-N curves) of the porous scaffolds filled with polymeric materials were also determined.

2. MATERIALS AND METHODS

2.1. Materials and manufacturing

Porous cylindrical samples were made of Ti-6Al-4V powders using a selective laser melting machine (Realizer SLM-125). Cubic diamond geometry with strut size of 433 μm was considered as the basic unit cell of the lattice structure (Figure 1). The metal powder was processed on top of a solid metal substrate in an inert atmosphere. All the samples had the diameters of 15 mm and the length of 20 mm. The porous Ti-6Al-4V cylinders were made in three different densities of $668.36\ kg/m^3$ (porosity =85%), $834.28\ kg/m^3$ (porosity = 81%), and $1002.9\ kg/m^3$ (porosity = 77%). Relative density was defined as the volume occupied by the titanium material divided by the total volume of the sample. To investigate the effect of the relative density of porous structures on the mechanical properties of both filled and unfilled structure, the porous structures with the abovementioned densities were filled by epoxy (Figure 2). To study the effects of the mechanical properties of the filler, the porous structures with the lowest relative density were then filled by epoxy, crystal clear Polyurethane (PU) resin (Smooth-On crystal clear 202), white PU resin (FormCast Rhino), and black urethane resin (Smooth-Cast ONYX®) to simulate ingrowth of bone (Figure 2) at various stages of maturation. To verify that the porous structures are completely filled by different fillers, several sections were made in different positions of samples filled by any type of filler. To determine the mechanical properties of the fillers, some cylindrical samples were made from the four noted materials and tested under compressive mechanical loading (Table 1 and Figure 3).

2.2. Mechanical testing

Each sample type was first tested under static loading to find its elastic modulus and yield stress. The static tests were done in accordance to ISO 13314:2011. To test the samples, an Instron

10000 ElectroPulse dynamic mechanical test machine with a 10kN load cell was used. The displacement rate was set to 1.5 mm/min. The elastic modulus E was obtained by measuring the slope of the stress-strain curve in the linear part between the two stresses σ_{20} and σ_{70} which correspond to the 20% and 70% of the plateau stress σ_{pl}, respectively. The yield stress σ_y was obtained by offsetting the linear part of the stress-strain curve by 0.2% of strain to right and measuring its intersection with stress-strain curve.

Compression-compression fatigue tests were done on the samples using the same machine used for the static tests. Sinusoidal wave shape with a frequency of 15 Hz was used for all the samples. A constant load ratio (i.e. the ratio of the minimum to maximum loads in each cycle) of $R = 0.1$ was used. To obtain the S-N curve for each sample type, the maximum applied load was varied (between $0.2\,\sigma_y$ and $0.8\,\sigma_y$ of the sample obtained from static tests) and the fatigue life was obtained for each loading level. The specimens were assumed to have failed once their stiffness dropped to 10% of their initial value. For each load level, two fatigue tests were done. In case the difference between the obtained lives of the two tests was more than 40%, a third test was carried out. For each sample type, an S-N curve was established using the data points corresponding to the applied stress level and the resulted fatigue lives. An exponential power-law was fitted to the data points of the S-N curves.

2.3. Numerical modelling

In order to observe the effect of filling the porous structure with different types of fillers on the stress distribution of the porous structure, numerical simulations were carried out using finite element method (FEM). The general static solver of ABAQUS was used to model the static elastic deformation of unfilled and filled structures. Three types of fillers (white PU resin, epoxy, and black urethane resin) with elastic moduli of 0.704, 1.136, and 1.52 GPa were considered for

numerical analysis. The size of the unit cells was similar to that in the additively manufactured porous structures (i.e. 1×1×1 mm^3). For meshing both the solid part and the filling part, the global mesh size of 0.065 mm was used. To mesh the structures, quadratic 3D-stress tetrahedral elements from ABAQUS standard library were used. All the nodes in the lowermost part of the structures were constrained in all the direction. The nodes located in the uppermost part of the structure were moved downward for 2% strain and they were constrained in the directions parallel to the upper grip. The structure size analysis showed that the stiffness of the lattice structure (either it is filled or not) converges for lattice structure sizes larger than 3×3×3, therefore this size of lattice structure was considered for all the simulations.

3. RESULTS

White PU resin, crystal-clear PU resin, epoxy, and black urethane resin respectively had the lowest to highest mechanical properties (Table 1 and Figure 3). The stress-strain curves of white and crystal-clear PU resins had three regions: initial linear elastic part, long plateau part, and final densification part. The stress-strain of epoxy was almost similar with the difference that its plateau part was very short. Regarding the black urethane resin, due to load limit of the load cells (10 kN), it was not possible to obtain the stress-strain curve in post-elastic region.

The elastic modulus and yield stress of the filled and unfilled structures increased with increasing the relative density of the porous structure (Figure 5). Moreover, filling the structure by any of the four fillers increased both the elastic modulus and yield stress of the porous structures (Figure 5). However, the increase in the noted properties was smaller for larger relative densities of the porous structures (Figure 5). The order of increase in the mechanical properties of the filled porous structures was in direct relationship with the corresponding material properties of the filler. The only exception was filling the structure with crustal clear PU resin which had the

lowest elastic modulus and yield stress among the fillers (Figure 4). The porous structures filled by crystal clear PU resin had the highest elastic modulus and the second highest yield stress among all the filled structures (Figure 5). Filling the porous structure by white PU resin increased the elastic modulus of the structure but did not have a significant effect on its yield stress (Figure 5).

At constant stress levels, increasing the relative density of the unfilled porous structure from 15% to 23% significantly increased the fatigue life of the structure (Figure 6a). Similarly, filling the porous structure with epoxy fillers drastically increased the fatigue life especially for the low-density porous structure (Figure 6a). For example, the endurance limit of the epoxy-filled low-density foam was about eight times of that in the unfilled structure. The difference between the endurance limits of the filled and unfilled structures in medium- and high-density foam was, however, smaller. For instance, the endurance limit of the filled high-density structure is less than three times of that of the unfilled structure. The S-N curves of the epoxy-filled structures with different relative densities were relatively closer to each other as compared to the S-N curves of similar structures when unfilled.

The S-N curves were normalized by dividing the stress by the yield stress of each structure type (Figure 6b). Comparison of the normalized S-N curves shows that filling the porous structure increases both absolute and normalized endurance limits (Figure 6). The normalized S-N curves of medium- and high-density porous structures were very close to each other for both filled and unfilled specimens (Figure 6b). Compared to medium- and high-density structures, the normalized S-N curves of the low-density porous structure were somehow higher (Figure 6b).

All strain-life diagrams showed a bi-stage curve (Figure 7). In the first stage, the strain was raised slowly with an increasing slope (Figure 7). After reaching a critical point, the strain was

increased very quickly and the sample failed in a very small number of cycles (Figure 7). Compared to the unfilled structures, the transition from the first stage to the second stage was much smoother in the epoxy-filled structures and took much more cycles (Figure 7). The failure strain in the epoxy-filled structures (about 2% strain) was also much larger compared to that of the unfilled structures (about 0.4% strain) (Figure 7).

For investigating the effect of other filler types on the fatigue response of porous structure, only the low-density porous structure was considered (Figure 8). Filling the porous structure with epoxy, PU, and urethane resins substantially increased the fatigue strength (Figure 8a). The S-N curves of the structures filled by white PU resin ($E_f = 0.704$), crystal clear PU resin ($E_f = 1.081$), and epoxy ($E_f = 1.136\,GPa$) were close to each other (Figure 8a). The structure filled by black urethane resin ($E_f = 1.52\,GPa$) showed a higher S-N curve than those of structures filled by the other resins (Figure 8a). The crystal-clear PU resin had higher yield stress than epoxy ($\sigma_{y,f} = 35.82\,MPa$ in PU resin compared to $\sigma_{y,f} = 31.8\,MPa$ in epoxy, Table 1). Therefore, both the fatigue resistance (Figure 8a) and static strength (Figure 5b) of the porous structures filled by PU resin were higher than those of the same structures filled by epoxy.

The failure mechanism in the unfilled structure and in the structures filled with different fillers was different. However, for each structure type, the failure mechanisms were similar for both static and fatigue loadings (Figure 9). All filled and unfilled structures failed after formation of a 45º failure band (Figure 9). While the unfilled structures only showed simple lateral expansion before their final failure (Figure 9a), the filled structures demonstrated various types of deformation shapes in stages preceding final failure (Figure 9b-f). The epoxy-filled structures exhibited barrel shapes (Figure 9b) and the crystal-clear PU-filled structures showed an inflated middle part (Figure 9d) before formation of the 45º failure bands. Most of the porous structures

filled by white PU resin showed double failure bands (both 45º) each one starting from one of the grip surfaces (Figure 9e).

The results of numerical simulations (Figure 10-11) showed that filling the porous structure by white PU resin (0.704 GPa), epoxy (1.136 GPa), and black urethane resin (1.52 GP) increases the maximum von-Mises stress in the porous structure from 1322 MPa to respectively 1678 MPa, 1567 MPa, and 1540 MPa (Figure 10). Therefore, filling the porous structure increases the maximum stress in the struts of the lattice structure (Figure 10). The interesting point is that for fillers with the elastic modulus values around 1 GPa, increasing the stiffness of the filler decreases the maximum stress in the porous structure (Figure 10). The maximum stress in the fillers was much lower than that in the solid parts (Figure 11). For example, by considering all the cases, it can be seen that the maximum stress in the solid parts is 1678 MPa (Figure 10), while the maximum stress in the filler is 138.9 MPa (Figure 11).

4. DISCUSSIONS

The results of this study show that full tissue regeneration inside the pores of additively manufactured porous biomaterials could have very large effects on both static and fatigue mechanical behavior of those bone substituting materials. The elastic modulus of the filler polymers used in this study ranged between 0.7 and 1.5 GPa, which is in the lower range of those observed for trabecular bone and generally lower than those of cortical bone [18-20]. Filling materials with these relatively low mechanical properties were selected to simulate the earliest stages of bone tissue regeneration where the bone tissue is not yet fully mineralized and mature. The earliest stages of *de novo* bone formation around bone substituting materials and implants [21] may involve woven bone which is mechanically inferior to lamellar bone. The progress of the mineralization process is also gradual. Since mineralization significantly influences the

mechanical properties of the bone tissue [22, 23], lower mechanical properties are expected in the earliest stages of bone regeneration. The results of this study show that even bone tissue with low mechanical properties could increase the overall mechanical properties of the bone-tissue complex such as elastic modulus and yield stress by a factor of 2-7 depending on the porosity of the biomaterial.

The results of finite element models showed that filling the porous structure with resins with stiffness values in the range of cancellous bone increases the maximum stress in the porous structures with smooth surfaces. This raise in the maximum stress can have negative effects on the fatigue behavior of porous structure. However, the results of our study showed that filling the porous structure actually improves the strength indicators of the materials including the yield stress and fatigue life (as compared to the elastic modulus that shows lower factors of increase in its value). This can be explained through the failure mechanism of additively manufactured porous biomaterials. The imperfections caused by the additive manufacturing such as variations in the diameter of the struts and notches [7, 11, 24, 25] could cause strain localization, local stress concentrations, and local buckling even when the porous structure is not experiencing buckling or plastic deformation at the macro-scale. Presence of a second phase such as regenerated bone tissue could play an instrumental role in delaying some of the above-mentioned contributors to failure such as buckling even when the mechanical properties of the second (soft) phase are much lower than those of the primary (i.e. hard) phase. This might be due to the fact that the soft phase distributes the applied load more uniformly throughout the outer surface of the struts and therefore relieves the high stress values experienced by the struts in more critical locations. When comparing yield stress and fatigue life, the fatigue life shows even larger percentages of improvement when polymers simulating fill the porous structures regenerated

bone tissue. That is due to the fact that even relatively small amount of load relief could push the loads experienced by (parts of the) the porous structure below the endurance limit, thereby increasing the fatigue life notably.

Even though the difference between the porosity of the structures considered in this study is limited to 8%, there is a large difference between the various porous structures in terms of the percentage of increase in their mechanical properties once they are filled with polymers simulating bone tissue regeneration. Porous structures with higher porosities generally gain much more as compared to those with lower porosities (for instance, 700% increase compared to 150% increase in terms of fatigue durability). There are least two primary mechanisms that could contribute to this observed behavior. First, structures with higher porosity simply have more pore space that could be filled with the infill materials such as de novo tissue (or its simulant). Second, porous structures with higher porosities generally have smaller strut dimensions. If the size of the imperfections caused by the additive manufacturing process could be assumed to be more or less constant, the same absolute size of imperfections influence the struts with smaller diameter much more than do influence those with larger diameter. The stress relieving effect of the filling material would then be more significant in the lower-density structures.

The results showed that increase in the elastic modulus and yield stress of the porous structure (Figure 5) has some relationships with the corresponding properties of the filler (Figure 4). There were, however, some exceptions. For example, while crystal clear PU resin had the lowest mechanical properties among the fillers, the elastic modulus and yield stress of the structure filled by it were the highest and the second highest ones among the structures filled by different fillers. Another exception was filling the porous structure with white PU resin which increased the elastic modulus of the porous structure but it decreased the yield stress of the structure. These

observed exceptions can be attributed to other influencing factors such as the degree of adherence of the filling material with the struts of the metallic porous structure, the post-yielding behavior of the filling material, and the deformation mode of the structures filled by different fillers (Figure 9).

Different resins caused deformation modes in the porous structures. In all the filled porous structures, the cross-section area of the cylindrical sample was not changed significantly in its contact surface with the grips (Figure 9). In the structures filled by epoxy, crystal-clear PU resin, and black urethane resin, the cross-section area of the middle part of the sample increased significantly before the 45° failure bands form (Figure 9). Similar to the unfilled structure, the structure filled by white PU resin did not show considerable increase in the cross-section area of its middle part (Figure 9c). This was because the shite PU resin has very small fracture strain (less than 5%). Fillers with larger fracture strains show more inflated regions in the middle part of the sample. In fact, the largest inflation in the filled sample before final fracture belongs to crystal-clear PU resin (Figure 9d), epoxy (Figure 9b), black urethane resin (Figure 9e), and white PU resin (Figure 9c) which respectively have fracture strains of 55%, 30.5%, 27.7%, and 4.8% (Figure 4). Therefore, it can be concluded that the most influencing parameter in the deformation mode of the infilled porous structure is the fracture strain of the filler. Cancellous bones have shown failure strains of about 75%. Therefore, it is expected that a porous structure with bone ingrowth tends to demonstrate very large degrees of inflation before final fracture, if it is not confined in the periphery, especially also due to the fact that bone has the intrinsic capability of self-curing. In-vitro or in-vivo tests can better shed light on what will happen in a porous structure. Most of the porous structures filled by white PU resin showed double failure bands each starting from one of the grip surfaces (Figure 9c). In the unfilled structures, there was

always one failure band which had also started from one of the grips (Figure 9a). In the unfilled porous structure, there might be also two failure planes with maximum stress levels. However, after the failure of the most critical plane of the unfilled structure, the damage area grows around that plane, since the struts located in that plane become increasing weaker after they are rubbed to the struts on the other side of the failure band. In the porous structure filled by white PU resin, the filling material might support the failed struts in the failure band letting the second failure band be formed.

Before carrying out this study, it could be predicted that filling the porous structure with different fillers would increase its mechanical properties. However, as a primary study, it was interesting to know that to what extent filling the porous structure can increase the static and fatigue behavior. One of the main findings of the study was that the increase is significant (for example endurance limit can be increased to values like 800%). The other finding was that compared to static properties, the fatigue properties are more enhanced after the porous structure is filled. Another finding was that the fracture strain is a very effective factor in determining the failure mechanism of the filled structure. Carrying out fatigue tests on porous structures with bone ingrowth is very expensive and time-taking. Moreover, depending on the location and percentage of bone ingrowth and the macro-geometry of the implant itself, the resulted mechanical properties can be significantly different. Considering different locations of bone ingrowth, different extents of bone ingrowth into the implant, bone tissue growth stage, etc. can create millions of scenarios for being studied which is out of the scope of this paper. To exclusively understand the effect of the porous structure porosity and density of the filler on the static and fatigue behavior of the porous structure and its deformation mechanism, it is better to decrease the possible scenarios (i.e.by considering 100% infill). Such as study is a primary step in

investigating the effect of bone ingrowth on the mechanical properties of the implant. In future studies, depending on the site the implant is going to be used for, the age of the patient, etc. (for example a femur head implant for a young male patient), relevant in-vitro tests can be carried out.

Although complete bone regeneration in additively manufactured porous biomaterials have been reported before [26], it should be noted that that tissue regeneration progress is gradual and not in all cases complete. The experiments performed here focused on the upper and lower bounds of the mechanical properties of additively manufactured porous biomaterials with the upper bound being the mechanical properties of the specimens with full bone regeneration (or fully filled with simulant polymer in the current study) and the lower bound being the mechanical properties of the as-manufactured porous structures. All partial cases of bone regeneration are expected to show mechanical properties in the range covered by the above-mentioned bounds. It is very challenging to determine the effect of partial tissue regeneration on the mechanical properties of additively manufactured porous biomaterials. It is therefore suggested that analytical [27, 28] or computational [11, 29] techniques be used for estimating the change in the mechanical properties of additively manufactured porous biomaterials caused by tissue regeneration.

Tissue regeneration into additively manufactured porous biomaterials might have more consequences than just increasing the mechanical properties of the implant. In a number of surgical techniques that are used for treatment of (segmental) bone defects, mechanical load is distributed between the implant and a fixation plate that anchors the porous biomaterial in place (see e.g. Figure 12). The musculoskeletal load is therefore divided through the fixation plate and the porous biomaterial. A number of studies have shown that at least for some of such constructions, the mechanical load going through the implant is dependent on its stiffness and

increases as the stiffness of the implant increases [30, 31]. Since the results of the current study show large increases in the mechanical properties of the bone-implant complex, the portion of the musculoskeletal load going through the implant is expected to increase as the tissue regeneration process progresses. Given the fact that mechanical loading plays an important role in tissue growth and remodeling [32-35], the bone regeneration process is expected to benefit from the increased mechanical properties of the bone-implant complex. It is therefore suggested that the surgical techniques are designed such that, similar to what is seen in the animal model depicted in Figure 12, the share of musculoskeletal loading going through the implant increases with increased stiffness of the implant.

One major aspects of the tissue regeneration process, i.e. biodegradation of the implant, was not considered in the current study. Biodegradation of additively manufactured porous biomaterials could work in a direction opposite to that of tissue regeneration and gradually decrease the mechanical properties of those materials. However, additively manufactured porous biomaterials made from biodegradable metals such as magnesium are relatively underdeveloped and the vast majority of studies focus on additively manufactured porous titanium or tantalum that are considered to be very close to clinical applications as compared to biodegradable materials.

5. CONCLUSIONS

The effects of bone tissue regeneration on the mechanical behavior of additively manufactured porous biomaterials were studied using polymeric filler materials whose mechanical properties were in the lower range of the mechanical properties expected for *de novo* bone tissue. Both static and fatigue life of the porous biomaterials drastically increased by factors 2-7 even when the porous biomaterial was filled with simulant materials with relatively low mechanical properties. The relative increase in the fatigue life was more pronounced as compared to the

increase observed for the static mechanical properties. Moreover, structures with higher porosities showed higher levels of increase in their mechanical properties as compared to less porous structures. These large values of increase in the mechanical properties of porous biomaterials with the progress of bone tissue regeneration not only have consequences for the load-bearing capability of bone-implant constructs, but may also change the loading conditions experienced by the construct with time and need to be further explored. Porous structures filled by different fillers showed different deformation modes before final fracture (when 45° failure bands form). It was seen that the larger the fracture strain of the filler material is, the more inflated the middle part of the porous structure would be before it is completely fractured.

REFERENCES

[1] Zadpoor AA. Bone tissue regeneration: the role of scaffold geometry. Biomaterials science 2015;3:231-45.
[2] Bose S, Vahabzadeh S, Bandyopadhyay A. Bone tissue engineering using 3D printing. Materials Today 2013;16:496-504.
[3] Derby B. Printing and prototyping of tissues and scaffolds. Science 2012;338:921-6.
[4] Ahmadi S, Campoli G, Yavari SA, Sajadi B, Wauthlé R, Schrooten J, et al. Mechanical behavior of regular open-cell porous biomaterials made of diamond lattice unit cells. Journal of the mechanical behavior of biomedical materials 2014;34:106-15.
[5] Arabnejad S, Johnston RB, Pura JA, Singh B, Tanzer M, Pasini D. High-strength porous biomaterials for bone replacement: A strategy to assess the interplay between cell morphology, mechanical properties, bone ingrowth and manufacturing constraints. Acta biomaterialia 2016;30:345-56.
[6] Takaichi A, Nakamoto T, Joko N, Nomura N, Tsutsumi Y, Migita S, et al. Microstructures and mechanical properties of Co–29Cr–6Mo alloy fabricated by selective laser melting process for dental applications. Journal of the mechanical behavior of biomedical materials 2013;21:67-76.
[7] Amin Yavari S, Ahmadi S, van der Stok J, Wauthlé R, Riemslag A, Janssen M, et al. Effects of bio-functionalizing surface treatments on the mechanical behavior of open porous titanium biomaterials. Journal of the mechanical behavior of biomedical materials 2014;36:109-19.
[8] Zhang S, Wei Q, Cheng L, Li S, Shi Y. Effects of scan line spacing on pore characteristics and mechanical properties of porous Ti6Al4V implants fabricated by selective laser melting. Materials & Design 2014;63:185-93.
[9] Amin Yavari S, Ahmadi S, Wauthle R, Pouran B, Schrooten J, Weinans H, et al. Relationship between unit cell type and porosity and the fatigue behavior of selective laser melted meta-biomaterials. Journal of the mechanical behavior of biomedical materials 2015;43:91-100.
[10] Zhao S, Li S, Hou W, Hao Y, Yang R, Misra R. The influence of cell morphology on the compressive fatigue behavior of Ti-6Al-4V meshes fabricated by electron beam melting. Journal of the mechanical behavior of biomedical materials 2016;59:251-64.
[11] Campoli G, Borleffs M, Amin Yavari S, Wauthle R, Weinans H, Zadpoor AA. Mechanical properties of open-cell metallic biomaterials manufactured using additive manufacturing. Materials & Design 2013;49:957-65.
[12] SU X-b, YANG Y-q, Peng Y, SUN J-f. Development of porous medical implant scaffolds via laser additive manufacturing. Transactions of Nonferrous Metals Society of China 2012;22:s181-s7.
[13] Lipinski P, Barbas A, Bonnet A-S. Fatigue behavior of thin-walled grade 2 titanium samples processed by selective laser melting. Application to life prediction of porous titanium implants. Journal of the mechanical behavior of biomedical materials 2013;28:274-90.
[14] Leuders S, Thöne M, Riemer A, Niendorf T, Tröster T, Richard H, et al. On the mechanical behaviour of titanium alloy TiAl6V4 manufactured by selective laser melting: Fatigue resistance and crack growth performance. International Journal of Fatigue 2013;48:300-7.
[15] Barriuso S, Chao J, Jiménez J, García S, González-Carrasco J. Fatigue behavior of Ti6Al4V and 316 LVM blasted with ceramic particles of interest for medical devices. Journal of the mechanical behavior of biomedical materials 2014;30:30-40.
[16] Hedayati R, Sadighi M, Mohammadi-Aghdam M, Zadpoor AA. Computational prediction of the fatigue behavior of additively manufactured porous metallic biomaterials International journal of fatigue 2016;84:67–79.
[17] Hollister SJ. Scaffold design and manufacturing: from concept to clinic. Advanced Materials 2009;21:3330-42.
[18] Reilly DT, Burstein AH. The elastic and ultimate properties of compact bone tissue. Journal of biomechanics 1975;8:393IN9397-396IN11405.
[19] Rho J, Hobatho M, Ashman R. Relations of mechanical properties to density and CT numbers in human bone. Medical engineering & physics 1995;17:347-55.

[20] Rho J-Y, Kuhn-Spearing L, Zioupos P. Mechanical properties and the hierarchical structure of bone. Medical engineering & physics 1998;20:92-102.
[21] Berglundh T, Abrahamsson I, Lang NP, Lindhe J. De novo alveolar bone formation adjacent to endosseous implants. Clinical oral implants research 2003;14:251-62.
[22] Currey J. Effects of differences in mineralization on the mechanical properties of bone. Philosophical Transactions of the Royal Society of London B: Biological Sciences 1984;304:509-18.
[23] Martin R, Boardman D. The effects of collagen fiber orientation, porosity, density, and mineralization on bovine cortical bone bending properties. Journal of biomechanics 1993;26:1047-54.
[24] Ahmadi SM, Yavari SA, Wauthle R, Pouran B, Schrooten J, Weinans H, et al. Additively manufactured open-cell porous biomaterials made from six different space-filling unit cells: The mechanical and morphological properties. Materials 2015;8:1871-96.
[25] Amin Yavari S, Wauthlé R, Böttger AJ, Schrooten J, Weinans H, Zadpoor AA. Crystal structure and nanotopographical features on the surface of heat-treated and anodized porous titanium biomaterials produced using selective laser melting. Applied Surface Science 2014;290:287-94.
[26] van der Stok J, Koolen M, de Maat M, Yavari SA, Alblas J, Patka P, et al. Full regeneration of segmental bone defects using porous titanium implants loaded with BMP-2 containing fibrin gels. European cells & materials 2015;2015:141-54.
[27] Hedayati R, Sadighi M, Mohammadi-Aghdam M, Zadpoor AA. Mechanics of additively manufactured porous biomaterials based on the rhombicuboctahedron unit cell. Journal of the Mechanical Behavior of Biomedical Materials 2016;53:272–94.
[28] Hedayati R, Sadighi M, Mohammadi-Aghdam M, Zadpoor A. Mechanical behavior of additively manufactured porous biomaterials made from truncated cuboctahedron unit cells. International Journal of Mechanical Sciences 2016;106:19-38.
[29] Eshraghi S, Das S. Mechanical and microstructural properties of polycaprolactone scaffolds with one-dimensional, two-dimensional, and three-dimensional orthogonally oriented porous architectures produced by selective laser sintering. Acta Biomaterialia 2010;6:2467-76.
[30] Amin Yavari S, van der Stok J, Ahmadi S, Wauthlé R, Schrooten J, Weinans H, et al. Mechanical analysis of a rodent segmental bone defect model: The effects of internal fixation and implant stiffness on load transfer. Journal of biomechanics 2014;47:2700-8.
[31] Poelert S, Campoli G, Van der Stok J, Amin Yavari S, Weinans H, Zadpoor A. Relating the microstructure of ti foam to load distribution and induced bone ingrowth. Journal of Biomechanics 2012;45:S334.
[32] Duncan R, Turner C. Mechanotransduction and the functional response of bone to mechanical strain. Calcified tissue international 1995;57:344-58.
[33] Huiskes R, Ruimerman R, Van Lenthe GH, Janssen JD. Effects of mechanical forces on maintenance and adaptation of form in trabecular bone. Nature 2000;405:704-6.
[34] Tanck E, Hannink G, Ruimerman R, Buma P, Burger EH, Huiskes R. Cortical bone development under the growth plate is regulated by mechanical load transfer. Journal of anatomy 2006;208:73-9.
[35] Zadpoor AA, Campoli G, Weinans H. Neural network prediction of load from the morphology of trabecular bone. Applied Mathematical Modelling 2013;37:5260-76.

List of figure captions

Tables

Table 1- Mechanical properties of bulk materials

Material	*Density* (kg/m^3)	*Elastic modulus* (GPa)	*Yield stress* (MPa)
Ti-6Al-4V	4430	122.1	980
Epoxy (1:1)	1149	1.136 ± 0.0056	31.8 ± 0.122
Crystal clear PU resin (0.9:1)	1036	1.081 ± 0.0087	35.82 ± 0.388
White PU resin	1065	0.704 ± 0.134	24.53 ± 1.4
Black urethane resin	1101	1.52 ± 0.118	44.35 ± 2.08

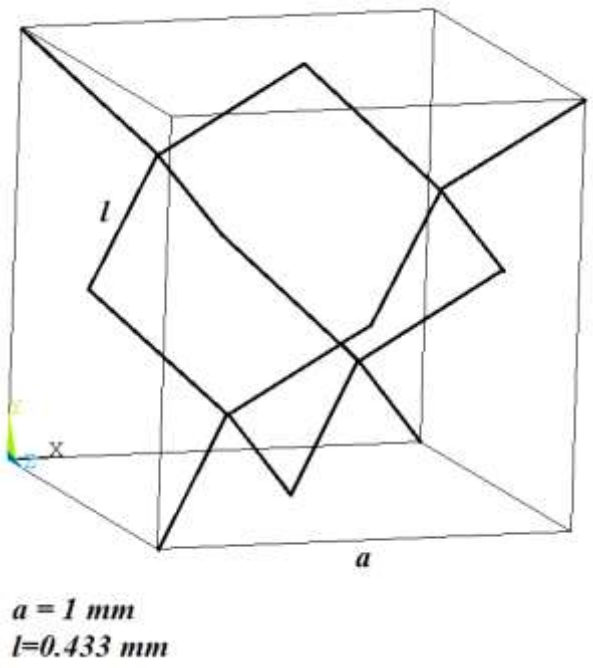

Figure 1- The diamond unit cell (the bold lines) used for creating the micro-scale geometry of the lattice structure and the related dimensions

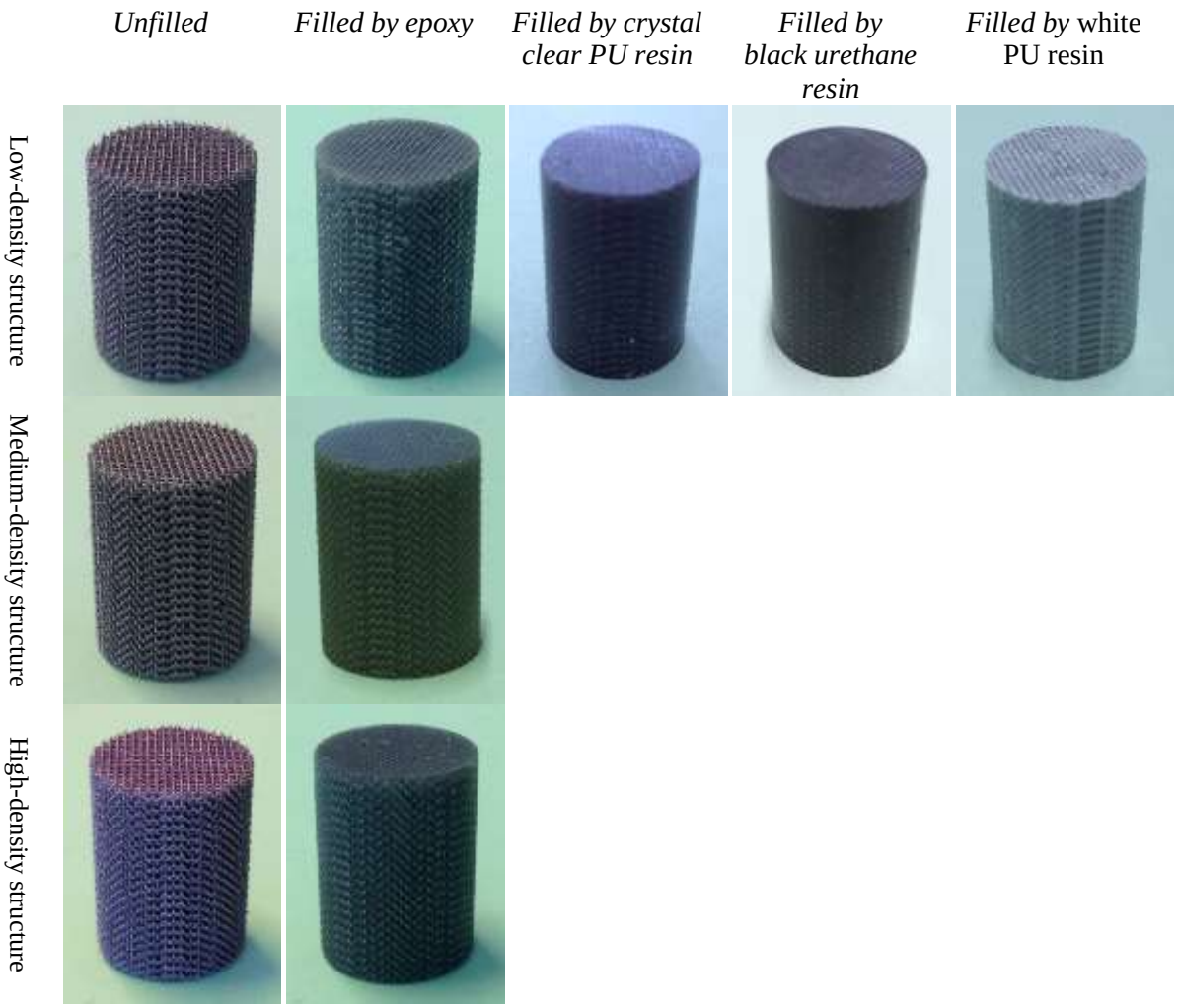

Figure 2- The unfilled and filled cylindrical samples

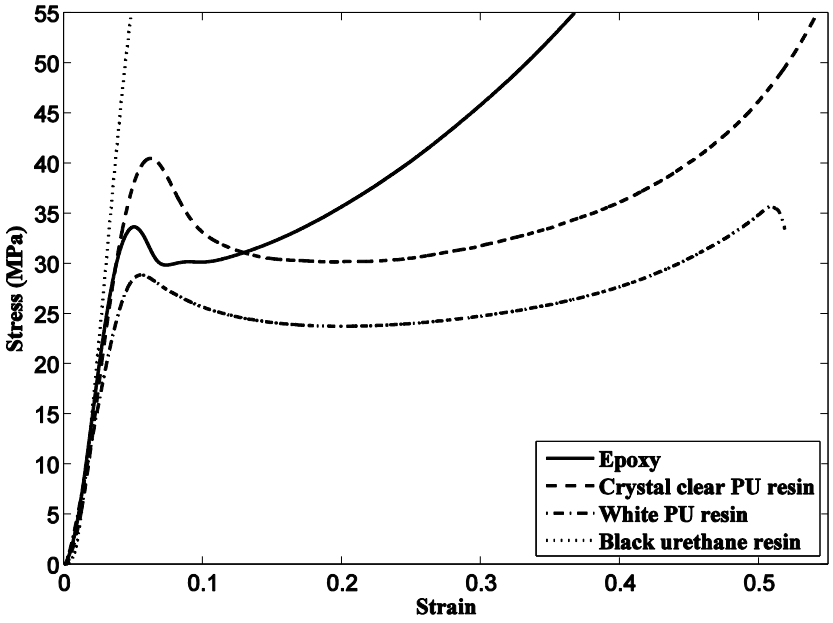

Figure 3- Stress-strain curves of materials used for filling the porous structure

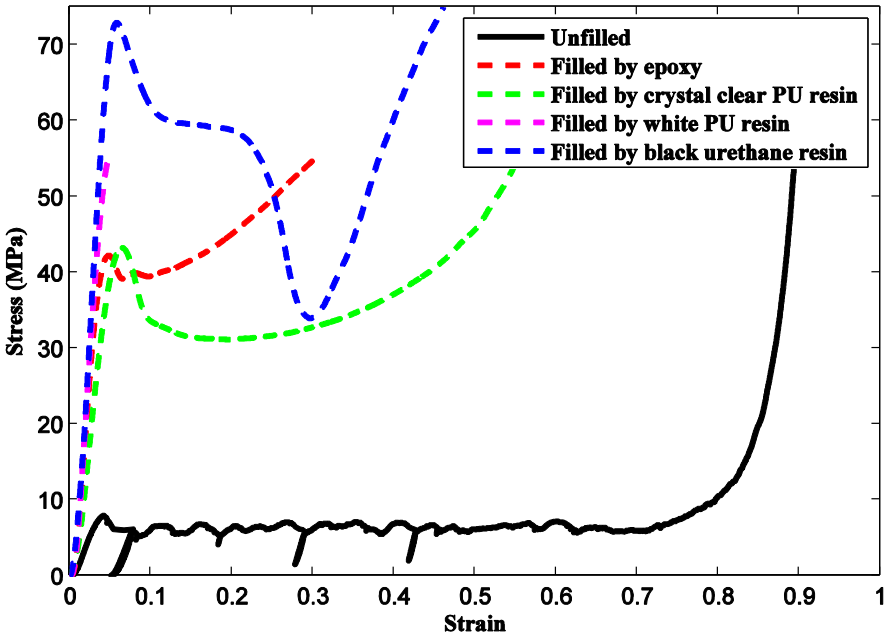

Figure 4- Stress-strain curves of low-density unfilled porous structure and low-density porous structures filled by different filling materials

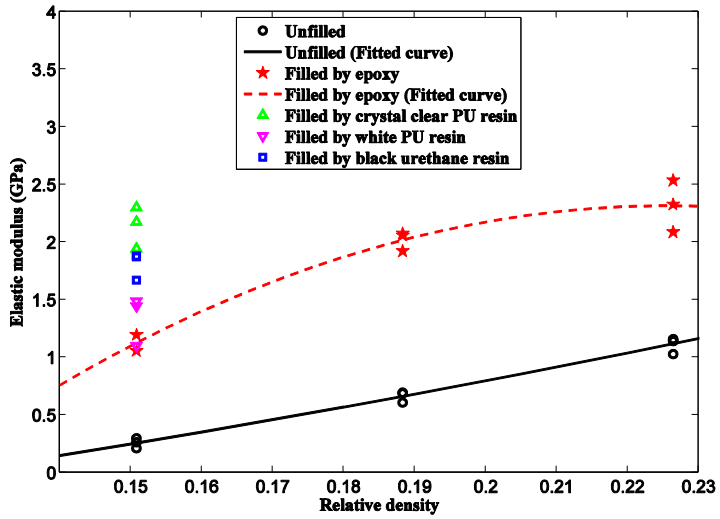

(a)

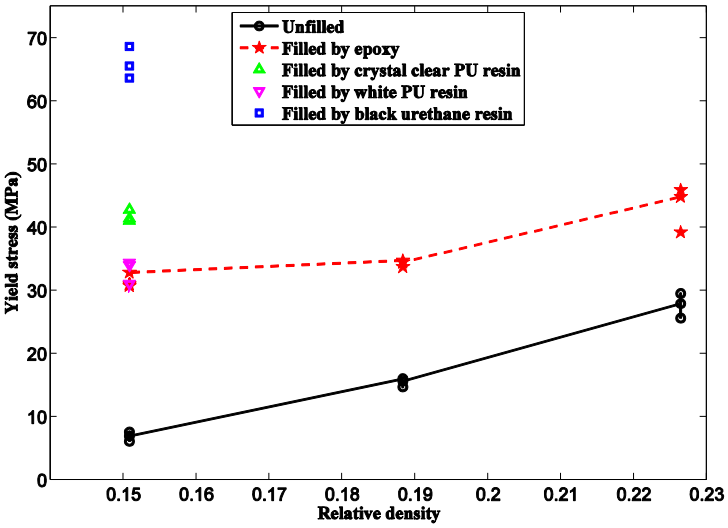

(b)

Figure 5- Comparison of (a) elastic modulus and (b) yield stress of unfilled and filled porous structures

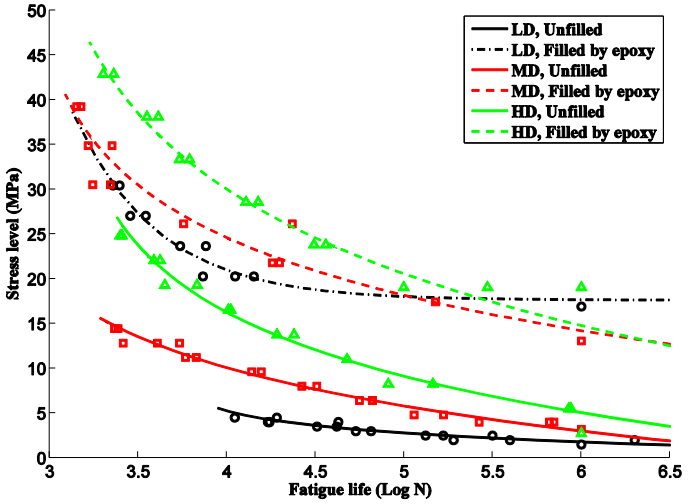

(a)

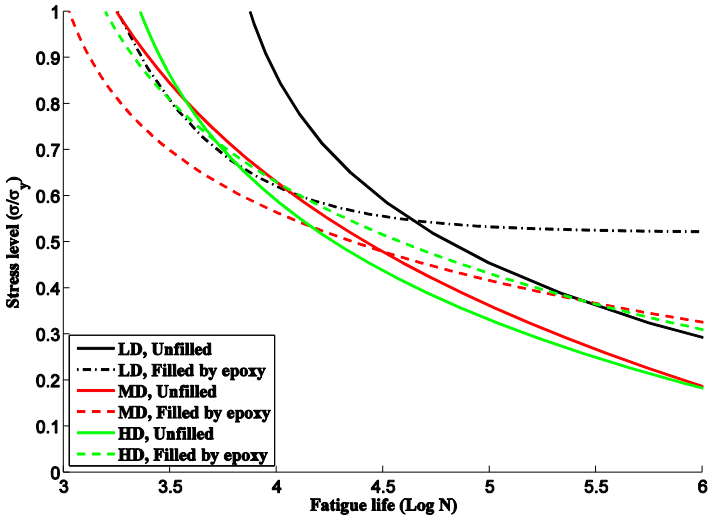

(b)

Material	*a*	*b*	*c*
LD- Unfilled	3.67201098	6.374564589	3.451755512
LD-Filled by epoxy	0.521511962	456.9975263	2.109116241
MD- Unfilled	2.537797062	4.988485296	1.949035235
MD-Filled by epoxy	2.840873233	12.48311757	4.210913298
HD- Unfilled	3.062235659	4.919959762	2.810323499
HD-Filled by epoxy	2.822468957	8.328541112	3.105794053

(c)

Figure 6- Comparison of (a) absolute S-N curves, (b) normalized S-N curves, and (c) constants of the S-N curves in the relationship $S = a + b\, e^{-c\, LogN}$ between unfilled and epoxy-filled cylindrical porous samples (LD, MD, and HD stand for low-density, medium-density, and high-density porous structures). The samples that were not failed after reaching 1,000,000 cycles are represented by filled markers

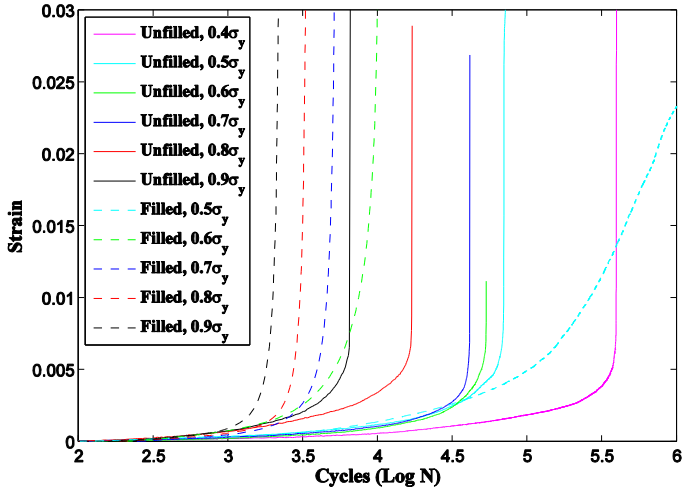

(a)

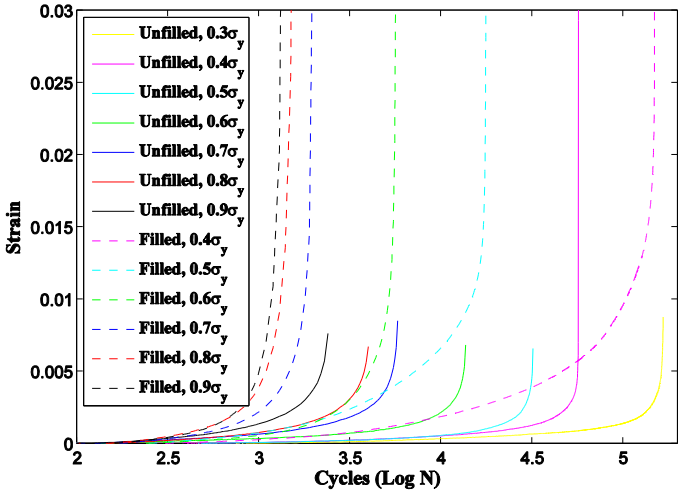

(b)

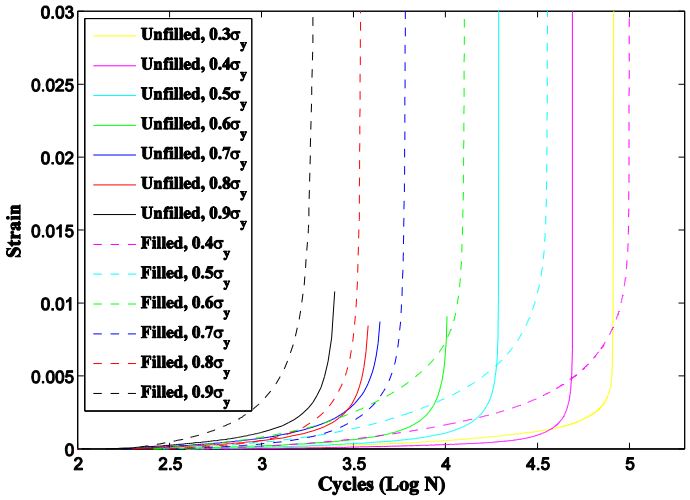

(c)

Figure 7- Strain-N curves of unfilled and epoxy-filled (a) low-density, (b) medium-density, and (c) high-density porous structures

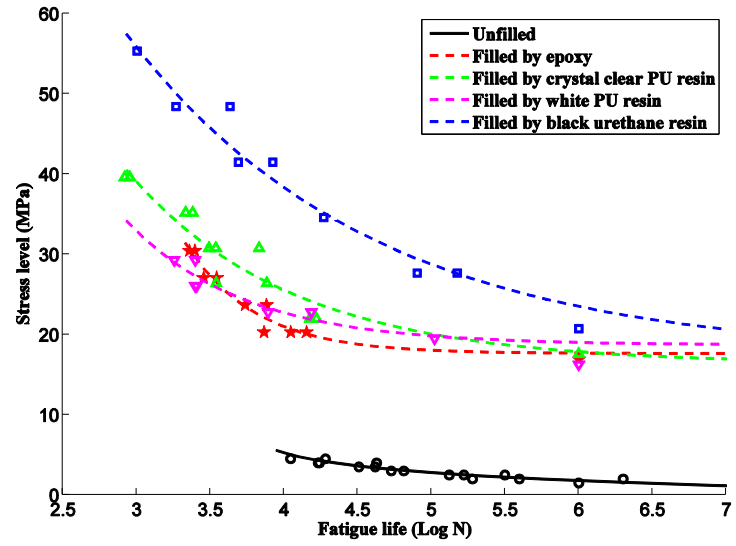

(a)

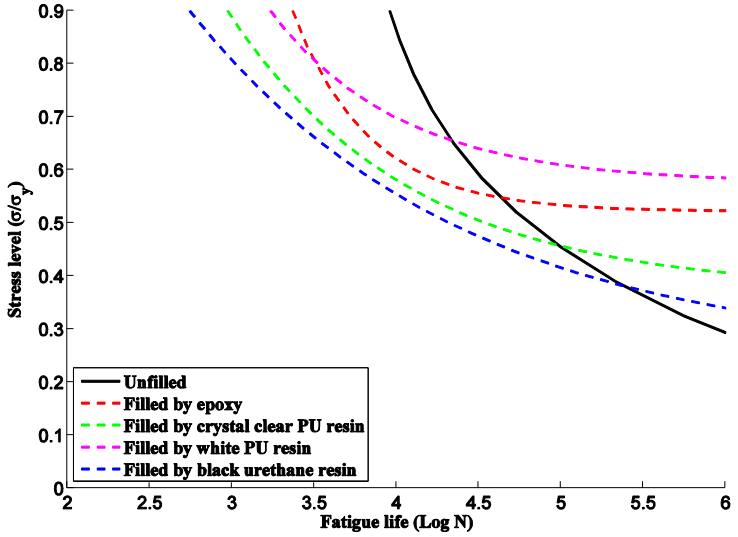

(b)

Filler	*a*	*b*	*c*
None	3.67201098	6.374564589	3.451755512
Epoxy	0.521511962	456.9975263	2.109116241
Crystal-clear PU resin	16.35933567	339.5125153	0.902303895
White PU resin	18.70618276	623.2855173	1.261054711
Black urethane resin	17.18350721	235.2001279	0.602346803

(c)

Figure 8- Comparison of (a) absolute S-N curves, (b) normalized S-N curves, and (c) constants of the S-N curves in the relationship $S = a + b\, e^{-c\, LogN}$ in porous structure with different fillers (The samples that were not failed after reaching 1,000,000 cycles are represented by filled markers).

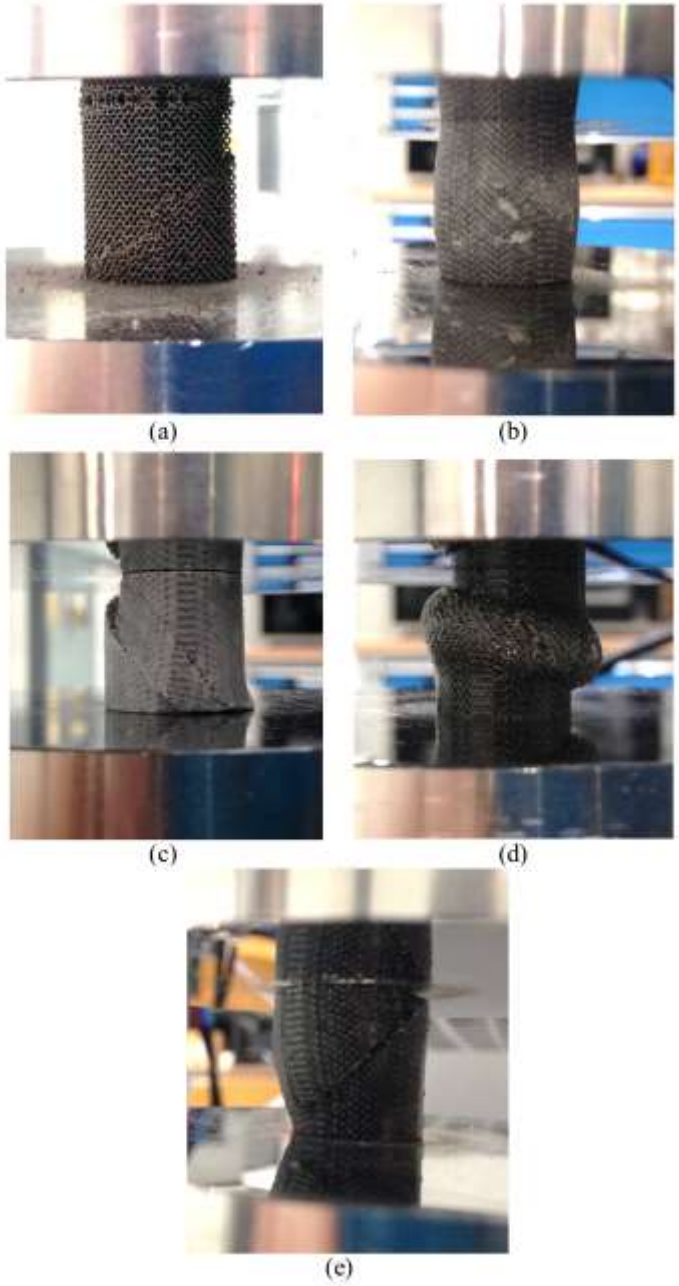

Figure 9- Failure modes observed in (a) unfilled samples, (b) samples filled by epoxy, (c) samples filled by white PU resins, (d) samples filled by crystal clear PU resins, and (e) samples filled by black urethane resin in static compression tests

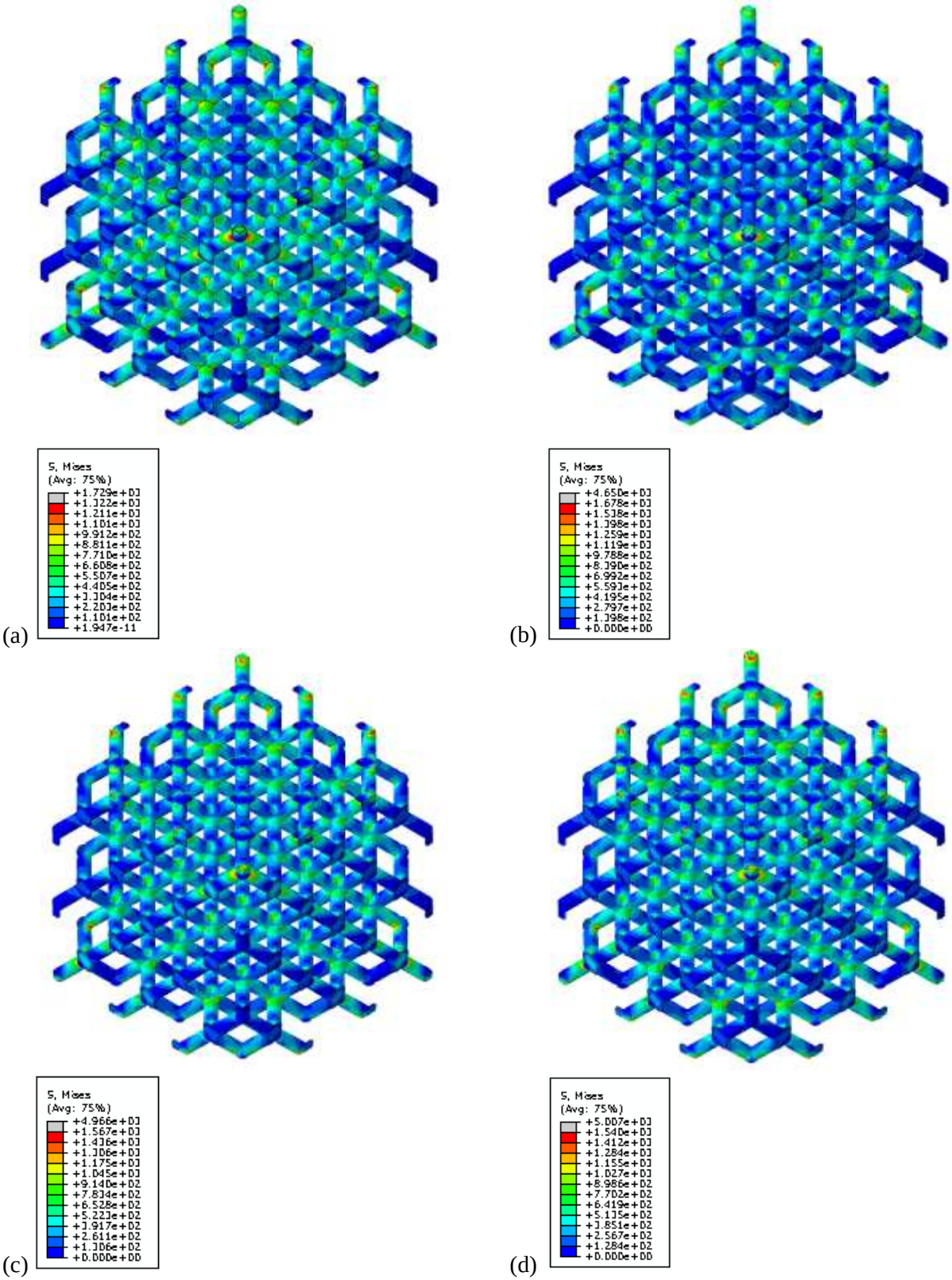

Figure 10- The stress distribution of (a) unfilled Ti-6Al-4V porous structure, and Ti-6Al-4V porous structures filled by (b) white PU resin, (c) epoxy, and (d) black urethane resin.

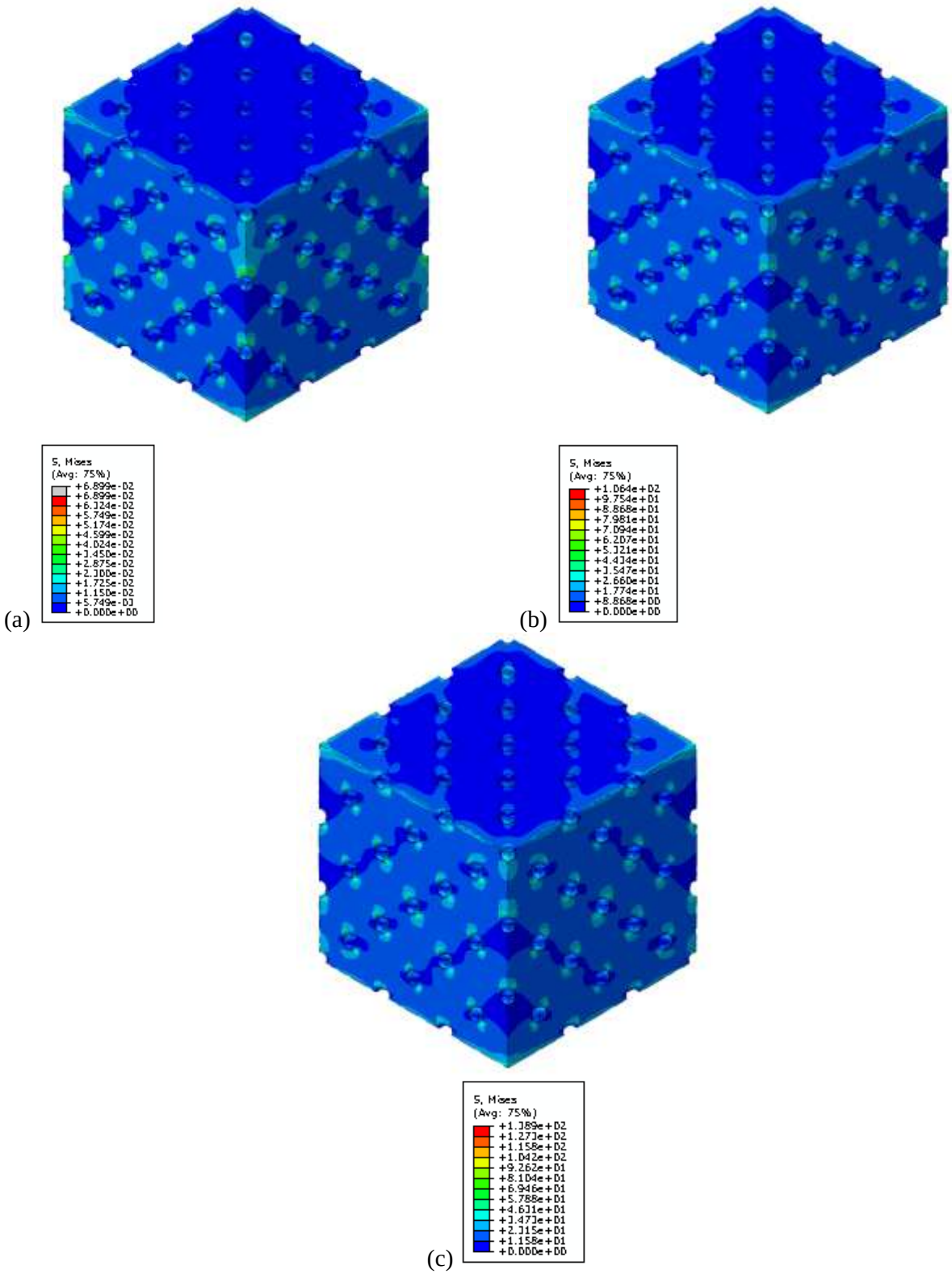

Figure 11- The stress distribution of different fillers: (a) white PU resin, (b) epoxy, and (c) black urethane resin

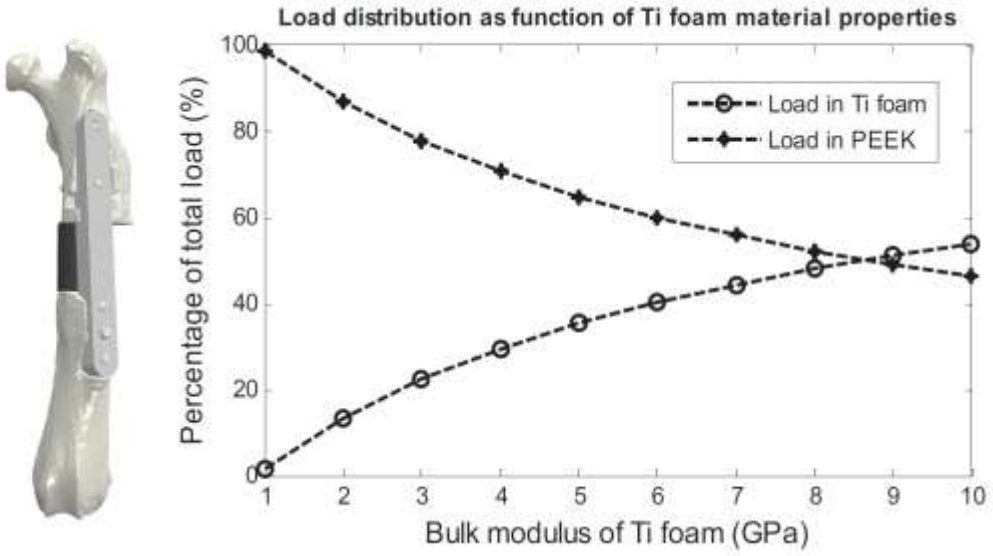

(a) (b)

Figure 12- (a) The FE model of a titanium plate attached to a rat femur and a porous titanium implant (b) The effect of change in the porous implant density on the load shared between the plate and the implant. Reprinted from [31], Copyright (2012), with permission from Elsevier.